Morphology of a Stream Flowing Down an Inclined Plane. Part 2: Meandering

1

Morphology of a Stream Flowing Down an Inclined Plane. Part 2: Meandering

B. BIRNIR[1], K. MERTENS[2], V. PUTKARADZE[2,3], AND P. VOROBIEFF[3]

[1]Department of Mathematics, University of California, Santa Barbara, CA 93106, USA

[2]Department of Mathematics, Colorado State University, Fort Collins, CO 80235, USA

[3]Department of Mechanical Engineering, The University of New Mexico, Albuquerque, NM 87131, USA

A stream of fluid flowing down a partially wetting inclined plane usually meanders, unless the volume flow rate is maintained at a highly constant value. However, fluctuations in the flow rate are inevitable in naturally occurring flows. Previous studies have conjectured that for some surfaces the meandering of a stream is an inherent instability. In this paper we show that on an acrylic plate we can eliminate the meandering by reducing perturbations entering the flow. By re-introducing controlled fluctuations, we show that they are indeed responsible for the onset of the meandering. We derive a theoretical model for the stream shape from first principles, which includes stream dynamics and forcing by external noise. While the deviation $h(x)$ from a straight linear stream $h(x) = 0$ shows considerable variability as a function of downstream distance x, when an ensemble average is computed, averaging power spectrum $S(k)$ as a function of wavenumber k for several different times t we obtain the power-law scaling $S(k) \sim k^{5/2}$. In addition, the growth of the area $A(x)$ swept by the stream at the distance x grows as $A(x) \sim x^{1.75}$.

1. Introduction

The scientific interest towards stream meandering in laboratory is in part driven by its apparent visual similarity to the river meanderings. River meanderings are influenced by many highly complex phenomena, which are difficult to control: turbulence in the water, soil erosion on the riverbed, variability of the soil properties, seasonal variations of the flow rate, *etc.* It is not clear at present which specific phenomenon contributes most to the river meandering, since all of them are highly intertwined. Two approaches to modeling of river meandering exist. First, there are derivations of dynamical equations based on first principles (Leopold & Wolman 1960; Ikeda *et al.* 1981); refer to Seminara (2006) for a recent and thorough review. Second, there is a stochastic approach with noise simulating the effects of turbulence and landscape variations. The works of Birnir (2007) and Birnir *et al.* (2007) offer some recent examples of this approach.

With the rivers as motivation, rivulets meandering on a partially wetting surface (glass or specially fabricated plastics, *e.g.,* Mylar, or polyethylene terephthalate) have attracted much recent attention (Davis 1980; Weiland & Davis 1981; Le Grand-Piteira *et al.* 2006). In particular, Davis (1980) and Weiland & Davis (1981) studied the stability of a rivulet with a fixed contact line, a moving contact line with a fixed contact angle, and a moving contact line with the angles dependent smoothly on velocity. They concluded that for the fixed contact line, the straight rivulet is stable if the flow is slow enough. For the moving

2   *B. Birnir, K. Mertens, V. Putkaradze, and P. Vorobieff*

contact line with a fixed contact angle, the rivulet was unconditionally unstable. Finally, for the case the contact angle α depending *smoothly* on the transverse rivulet velocity v, the stability was found to depend strongly on the value of the derivative $d\alpha/dv$. This approach was further developed by Young & Davis (1987), who discussed the effects of contact line motion and slip at the surface affecting the stability. In addition, Culkin & Davis (1984) produced rivulets on different surfaces (including acrylic) and discussed the conditions for stability and instability using a model of slender rivulets with a high Reynolds number, where pressure gradients were generated by curvature, surface tension and contact-angle hysteresis balance (also see Kim *et al.* (2004)). Experiments and to some extent theories (Nakagawa & Scott 1984; Schmuki & Laso 1990; Nakagawa 1992) were interpreted to suggest the existence of a stability boundary, beyond which there is a bifurcation from stable to an unstable regime. Such stability boundaries of different regimes, as well as various quantities in a meandering stream on a Mylar plate (*e.g.*, the leading unstable wavelength), were recently assessed by Le Grand-Piteira *et al.* (2006). Again, this study deemed the contact-angle hysteresis to play a major role.

These works concentrate on the dynamical approach to this problem, treating meandering as an inherent instability of the fluid rivulet. Further development of the theory was strongly hampered by the complexity of the contact angle behavior (see deGennes (1985) for fundamental reference), with a complete theory of contact angle hysteresis unavailable to this day. Nevertheless, by the end of 1990s it seemed that the instability of the flow for high flow rates had been established and the problem was solved at least in principle. Three major conclusions were derived from earlier works. First, above a certain flow rate, meandering is inevitable, at least for some surfaces. Second, a dominant wavelength exists in the meandering regime. Third, a regime of *stationary* meandering is realized for parameter values different from the time-dependent meandering.

Then, there was a surprising (and largely unnoticed) work by Nakagawa & Nakagawa Jr. (1996) reporting the re-stabilization of the rivulets in the regimes presumed unstable. The formation of *braids* close to the stream origin was reported (the braids were called *beads of a rosary* in that original paper). Mertens *et al.* (2004, 2005) observed rivulet re-stabilization for a large range of values in the parameter space and fully explained braiding theoretically, finding the transition boundary between the braiding and the non-braiding regimes. Our subsequent experiments on an inclined acrylic surface put in further doubt the theory treating meandering as an inherent rivulet instability.

First, by eliminating flow rate disturbances, we can completely suppress the meandering for *all* parameter values attainable in our experiment. Re-introducing the disturbances back into the stream makes the stream meander; turning off the disturbances reliably stabilizes the stream. The stabilization is achieved easier for higher flow rates.

Second, we show that, while a large variety of meandering profiles is realized, the power spectrum of even a small data set of meandering flow fields shows a power-law behavior and thus rules out the existence of a dominant wavelength. In a sense, meandering is akin to turbulence, where all wavelengths are present.

Third, at flow rates attainable at our experiments (Reynolds number $500 - 18,000$), we were unable to produce repeatable observations of the stationary meandering regime.

Our experiments show the fluid meandering on a partially wetting smooth surface to be driven exclusively by disturbances in the flow. Thus it is necessary to use the stochastic approach to the problem, which is the object of the theoretical part of the paper and has not been considered before. There are two stochastic forces at work here: first, the flow rate disturbances that cause the meandering, and second, the forcing of the stream by droplets left on the surface by the previous meanderings. The final results of our theory depend on the presence of these droplets, but are independent of the exact nature of their
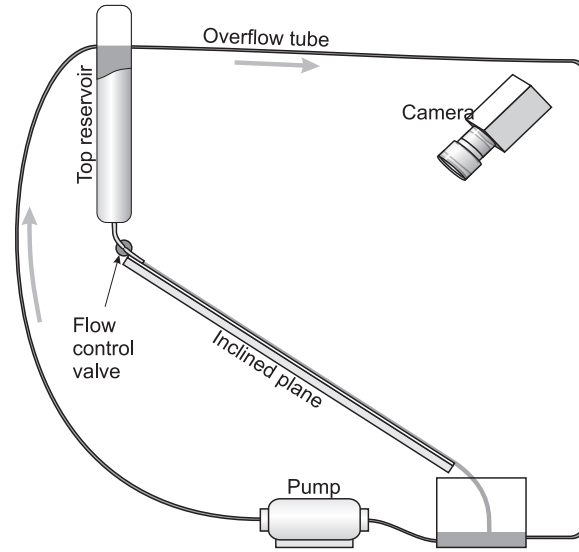
FIGURE 1. Schematic of the experimental arrangement.

distribution in the plane, as long as this distribution remains more or less uniform all the way downstream. This approach enables us to formulate the stochastic theory of this phenomenon explaining all the available experimental data with no fitting parameters.

While we make no explicit claim on the possibility of modeling rivers with our model for a stream on a partially wetting surface, we must nevertheless point out several uncanny similarities between the statistical properties of real-world rivers and streams in our laboratory: in this paper, we show that in the limit of very long streams, our modeling equations predict the meandering exponent of the stream to be 1/6, which coincides with that of rivers. We also show that the the growth of the basins of real rivers and of the streams in our experiments are described by exactly the same power law.

2. Experimental setup and observations

The experimental arrangement (Fig. 1) provides a highly constant discharge rate from a tall cylindrical top reservoir through a hole in its bottom connected to a flexible plastic tube. The diameter of this tube, and the hole, is $d = 3$ mm. The diameter of the container is $D = 15$ cm. Thus $d \ll D$, and the flow discharge rate Q is fairly well approximated by the formula originally introduced by Torricelli (Clanet 2000), $Q = \pi d^2/4\sqrt{2gZ}$, where g is acceleration due to gravity and Z is the height differential between the location of the hole and the free surface. Thus, if Z remains constant, $Q \equiv const$ as well. For a fixed tube diameter, Q can be altered by changing Z.

The flexible tube that carries the flow to the inclined plane is necessary to prevent any capillary instabilities that might form on the free surface of a water jet. An electronically controlled valve can alter the flow rate by squeezing the tube, thereby reducing its cross-section. The inclined plane is a produced by placing a large (2.4 m long and 1.2 m wide) sheet of acrylic plastic (3.2 mm thick) on top of a 2.4 m×1.2 m×2.5 cm urethane slab, which in turn is mounted on a welded–steel frame. This frame is attached to two pivots, with a screw arrangement controlling its angle of incline α with respect to the horizontal.

After the flow exits the tube, it runs down the incline and into a long rectangular bottom reservoir, from which it is recirculated with an electric pump connected to the

4   *B. Birnir, K. Mertens, V. Putkaradze, and P. Vorobieff*
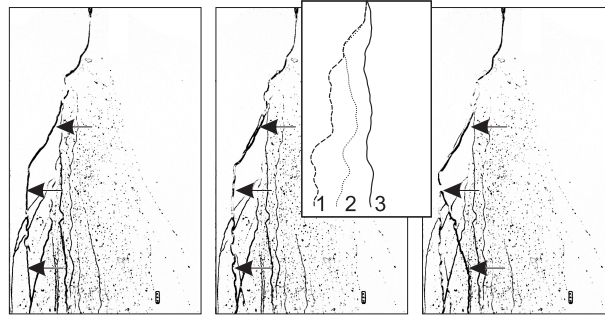

FIGURE 2. Time sequence of images (left to right) showing meandering flow. The images are processed with an edge-detection filter that emphasizes droplets deposited on the surface and makes it possible to observe both the current and the former rivulet paths. Arrows denote the current flow path. Interval between images is 7.5 s. Inset shows similar behavior of simulated meandering flow.

top reservoir. Note that the top and bottom reservoirs are also connected with an overflow tube, which ensures that the free surface of the top reservoir remains at a constant level.

Figure 2 shows the flow of water with trace amounts of food coloring, captured with a 4-megapixel grayscale digital camera mounted above the incline. The effective resolution of the images is about 1 mm per pixel. Any optical distortions are removed from these images as follows. An image of a rectangular grid is captured by the camera. This bitmapped image with any distortions is then mapped to the bitmap containing the undistorted image. The mapping procedure produces a bicubic spline mapping scheme which is then used to process the experimental images. Prior to each experimental run, a background image with no stream is captured, to be subtracted from the images showing the stream and the droplets left in the process of its meandering. Subsequently, the centerline of the stream is extracted from the processed images. Our conservative estimate of the cumulative error of the extraction and distortion correction for the centerline coordinates is on the order of one pixel (about 20 % of the characteristic stream width). The stream of fluid in this setup is highly controllable. After some initial settling time, the stream flowing down the plane assumes a straight shape for all the flow regimes we investigated. During the settling time, three distinct flow regimes could be observed: first, a region in the immediate downstream where stabilization had occurred, second, a region of continuous meandering, and third, a region where the stream breaks up. In the third regime, stream splitting events usually occur at the inflection points of the stream.

If the flow control valve remains open (no flow rate disturbances), the stream always stabilizes to the stationary non-meandering shape. Note that the long and narrow top reservoir stabilizing the flow is crucial for rivulet stabilization. If that reservoir is removed, or a flat and shallow reservoir is used (even having the same volume capacity), the meandering never stops due to the inherent disturbances introduced by the pump. Thus, careful attention to disturbances in the flow is imperative for this experiment.

The steady-state regime is described in our previous work, see Mertens *et al.* (2004, 2005). To destabilize the rivulet and produce continuous meandering, we added an electronically operated valve to our original flow system, introducing flow rate fluctuations at will, which destabilize the straight rivulet flow, producing meandering at all the attainable flow rates. When the valve is switched off, the stream always returns to the straight shape, although the relaxation time can be quite large for smaller flow rates. In a few cases where we observed a meandering pattern become stationary without straightening out (*stationary meandering* according to Le Grand-Piteira *et al.* (2006)), this effect could

always be attributed to the sedimentation of dirt and dust particles on the surface. Cleaning the surface and re-starting the experiment led to reemergence of the non-stationary meandering if flow rate disturbances were present in the flow. If the disturbances were absent, restarting the experiment produced a straight rivulet.

Some of the discrepancy between our findings and previous literature may be due to the difference in the surface wetting properties. It was noted by Le Grand-Piteira *et al.* (2006) that surface properties play a crucial role in this phenomenon. The presence of the droplets could explain an apparent discrepancy between our results and some earlier works, since the stream could deposit droplets in different fashions for different surfaces. Another possible explanation is the accumulation of electric charges on some surfaces that also may influence the flow dynamics in other experiments. We shall note, for all surfaces we have used (acrylic, Rain-X coated acrylic and polypropylene) the spectrum results reported in this paper are identical, although individual meandering profile as well as droplet distributions are drastically different.

3. Governing equations

Consider the flow of fluid on an inclined plane at an angle α with the horizontal. Let us define the (x, y) Cartesian coordinate system in this plane so that its origin coincides with the origin of the stream, and the $x-$axis is pointing straight downstream (*i.e.*, the centerline of a non-meandering rivulet will follow the $x-$axis). Then the momentum equation for the fluid in the rivulet can be written as

$$\frac{d\mathbf{U}}{dt} + \mathbf{U} \cdot \nabla \mathbf{U} = \frac{1}{\rho} \nabla P + g \sin \alpha \hat{e_x} + \nu \nabla^2 \mathbf{U} + \mathbf{H}, \tag{3.1}$$

where $\mathbf{U}$ is the fluid velocity vector, P is the pressure field, ρ the fluid density, ν its kinematic viscosity, α is the angle of the incline ($\alpha = 0$ for a horizontal plane), and $\hat{e_x}$ is the unit vector pointing downstream. $\mathbf{H}$ denotes additional forcing, whose nature may vary depending on the specific setting of the problem. The dominant contributions to the force balance come from the surface tension, friction on the bottom of the stream, and internal viscous dissipation, all of which work against fluid inertia and gravity.

We use the standard lubrication approximation to reduce the full three-dimensional equations with boundary conditions ($z-$axis being normal to the plane of the flow) to equations in two dimensions where the $z-$dependence is averaged out and the no-slip condition on the bottom is implicitly accounted for. A very similar technique has been described in detail in the first part of our paper. The lubrication approximation is based on the assumption that the vertical velocity profile in the fluid is parabolic, due to the non-slip boundary condition on the bottom of the stream, and the stress-free condition on the top (free surface). With these assumptions, we can show the $x-$component of the friction force to be $F_{f,x} = -3\nu u/l^2$, where u is the value of the $x-$component of velocity averaged in the z direction and l is the average stream depth. As the stream is narrow, we can safely assume that u does not vary much in the cross-stream direction. Thus we introduce single values of the velocity components ($\mathbf{U} = u\hat{e_x} + v\hat{e_y}$) in the $x-$ and $y-$directions for a given cross-section of the stream.

Let the stream discharge rate at a given location be $Q = Au$, where A is the cross-sectional area of the stream in the plane normal to the $x-$axis. Assume that the width of the stream is w. The simplest possible form of the equation describing the free surface ζ in this plane is parabolic, $\zeta = \frac{3}{2}l\left(1 - 4y^2/w^2\right)$ The area of this section is $A = lw$. Now, using $Q = Au = lwu$, we write the equation for the friction force as $F_{f,x} = -3\left(u^2w\right)/\left(Ql\right)$. The ratio w/l is actually related to the contact angle ϕ as follows. By evaluating $\partial\zeta/\partial y$

6   *B. Birnir, K. Mertens, V. Putkaradze, and P. Vorobieff*

at $y = -w/2$ (the edge of the stream), we find its value to be $6l/w$. But this slope equals $\tan \phi$. Thus $w/l = 6/\tan \phi$ and $F_{f,x} = -18u^2/(Q \tan \phi)$. By introducing a parameter $\lambda = 18\nu/(Q \tan \phi)$ and performing similar analysis for the $y-$component of the friction force, we can then write the following expressions for the components of the friction force in the two-dimensional formulation of the problem: $F_{f,x} = -\lambda u^2$ and $F_{f,y} = -\lambda uv$.

Next let us consider the pressure term, with the pressure to be inferred from the influence of surface tension. For this derivation, assume that the variation of the width of the stream $w(x,t)$ is sufficiently small that the width can be represented by its characteristic value w. In reality, the shape of the cross-sectional area of the stream changes with time, and the contact angle is subject to hysteresis. However, if we are dealing with gradual movement of the stream (characteristic contact-line velocities associated with meandering are much lower than $U = |\mathbf{U}|$), it is reasonable to assume that the variation of this shape is commensurately small, and so are the variations of w and l. For this and the subsequent derivations, we also regard the downstream velocity components as uniquely defined by the downstream distance x, as all the variations of velocity in the cross-section of the stream are either small enough to be irrelevant (in the $y-$direction) or have been averaged out (in the $z-$direction).

Let the deviation of the centerline of the stream from the $x-$axis be $h(x,t)$. For a straight rivulet, $h(x,t) \equiv 0$. Then the length of the centerline of the stream between downstream locations x_1 and x_2 is $L = \int_{x_1}^{x_2} \sqrt{1 + h_x^2} dx$, where $h_x = \partial h/\partial x$. For a contact angle characterizing a partially wetting surface ($\phi < 90°$), the stream is shallow ($l = w \tan \phi/6$). Thus the surface area of the stream between x_1 and x_2 is approximately the same as the wetted area

$$S = wL = w \int_{x_1}^{x_2} \sqrt{1 + h_x^2} dx$$

The surface tension will tend to minimize this surface area, thus the surface tension force per unit length is equal to $F_s = \gamma \delta S/\delta h$. Thus, the corresponding capillary force per unit volume is

$$\frac{F_s}{A} = \frac{F_s}{wl} = -\frac{\gamma}{l} \frac{\partial}{\partial x} \left(\frac{h_x}{\sqrt{1 + h_x^2}} \right).$$

Subsequently the component form of the equations of motion Eq. 3.1 takes the form:

$$\frac{\partial u}{\partial t} + u\frac{\partial u}{\partial x} = -\lambda u^2 + \frac{1}{A\rho}\frac{\delta S}{\delta h}\cos\theta + g\sin\alpha + \nu\frac{\partial^2 u}{\partial x^2} + \eta_x \qquad (3.2)$$

$$\frac{\partial v}{\partial t} + u\frac{\partial v}{\partial x} = -\lambda uv + \frac{1}{A\rho}\frac{\delta S}{\delta h}\sin\theta + \nu\frac{\partial^2 u}{\partial x^2} + \eta_y \qquad (3.3)$$

The terms containing λ are added as the result of our use of the lubrication approximation. Angle θ in the terms representing the components of the pressure (*i.e.*, surface tension) force is the angle between the direction of the stream and the $x-$axis, in other words, $\tan \theta = h_x$. The components of the random force $\mathbf{H}$ are $\eta_x = \eta \cos \theta$ and $\eta_y = \eta \sin \theta$. We must also add the continuity equation, which can be written in the form of a kinematic condition for $h(x,t)$:

$$\frac{\partial h}{\partial t} + u\frac{\partial h}{\partial x} = v \qquad (3.4)$$

The system (3.2 – 3.4) can be further simplified by considering the order of magnitude of various terms under the assumption that $v \ll u$. Then, $h_x \ll 1$ and the surface tension

term linearizes as follows:

$$\frac{\delta S}{\delta h} = -\frac{h_{xx}}{\sqrt{1 + h_x^2}} \simeq -h_{xx} \,. \tag{3.5}$$

An important part of the subsequent discussion is the structure of the noise term η. There are two possibilities. First, one can take $\eta(x,t)$ as a white noise with the correlation $< \eta(x,t)\eta(x',t') > = A\delta(x - x', t - t')$. This assumption leads to an analytical solution (in stochastic sense) for the system (3.2–3.4) under the assumption that the friction coefficient λ in (3.2,3.3) vanishes. The solution, interestingly enough, provides a meandering exponent of 1/6 corresponding to the real-world rivers. This solution is presented later in the paper.

However, assuming $\eta(x,t)$ to be white noise is not adequate for explanation of experimental results. Indeed, the white noise ansatz for $\eta(x,t)$ can only be assumed if there is a large number of droplets of random sizes distributed all over the length of the meandering stream, affecting it at all times. We believe that this assumption is correct for large-scale flows like rivers, where there is continuous random forcing on all scales. However, in our experiment at each given time instant the stream encounters only a very limited number of droplets. Thus, we use the assumption that $\eta(x,t)$ is a 'spike' appearing at a random sequence of times $t_1, \ldots t_n, \ldots$. At each time t_k, the position of the spike x_k is also chosen at random. We have tried several distributions of these droplets in space, and as long as they are not too skewed (*i.e.*, concentrated towards the beginning or the end of the stream), the results we report below do not change *for wavelengths corresponding to the scales larger than droplet size*. In addition, our results do not change depending on the shape of each droplet as long as it is localized. We have tried a rectangular pulse function of width l, inverse helmholtzian $\exp(-|x - x_k|/l)$ and Gaussian $\exp(-(x - x_k^2)/l^2)$. Note that in experiments, droplet size distribution changes with the substrate (Birnir *et al.* 2008), but all experimental droplet distributions on different substrates lead to exactly the same power spectra presented in Fig. 3.

Note that all the modeling results presented here assume uniform distribution of droplet times $t_1, \ldots t_n, \ldots$; for each time t_k the distribution of droplets x_k is uniform in space. The shape of the forcing is Gaussian, with width l equal to the cross-section of the stream (2 mm). Several examples of the profiles for the deviation from the centerline $h(x,t)$ are given at Fig. 2.

4. Quantitative analysis of experiments and comparison with theory

Our analysis of the stream presented here is based on 105 flow images on acrylic substrate acquired with a high-resolution computer-controlled digital camera (behavior of the flow on other partially wettable substrates is remarkably similar statistically, see Birnir *et al.* (2008)). The time intervals between the pictures were random and long enough for the flow patterns to be statistically independent. From each image at time t_m, we extracted the deviation of the stream from the centerline $h_m(x)$ as the function of downstream distance x. From members of the ensemble $h_m(x)$, $m = 1 \ldots 105$, we computed power spectra $S_m(k)$, where wavenumber $k = 2\pi/\lambda$ corresponds to a spatial wavelength λ. While the power spectra $S_m(k)$ based on single images are rather noisy, the spectrum produced by averaging over the ensemble $S(k)$ manifests a smooth graph with apparent power-law scaling $S(k) \sim k^{-5/2}$ over the span of about two decades (Fig. 3, left). Note that averaging over as few as 30 realizations from the ensemble produces a smooth graph with the same power-law exponent. Deviation from this scaling is noticeable only for $k \geqslant k_{max} \simeq 5cm^{-1}$, corresponding to physical scales smaller than the characteristic

8   *B. Birnir, K. Mertens, V. Putkaradze, and P. Vorobieff*

stream width. The largest physical scale we can acquire (and thus the smallest wavenumber) is constrained by the 2.4 m streamwise extent of our experimental arrangement. The scaling behavior is a persistent feature of all our experiments, representing a universal characteristic of the problem of the flow down a partially wetting incline. One important conclusion from the power law behavior is that the leading wavelength associated with meandering instability claimed by previous authors does not exist. The results were repeated for three surfaces: acrylic (contact angle $57 \pm 2°$) , acrylic with hydrophobic coating (contact angle $74 \pm 5°$) and polypropylene (contact angle $99 \pm 4°$). The results for spectra and "basin area" (see below) for these surfaces appear indistinguishable.

To compare the experimental results with our theory presented above in Sec. 3, we have performed numerical simulation of Eqs. (3.2-3.4) over a long time and computed an average of the spectrum for the deviation of centerline for an ensemble $h_m(x) = h(x, t_m)$ using a sequence of time points t_m. This spectrum is also presented in Fig. 3, left. The only fitting parameter is the normalization for noise strength $\eta(x, t)$, taken as a constant for all runs. Our theory faithfully reproduces the scaling behavior up to the largest physically relevant values of k corresponding to the droplet forcing width.

As another test of our theory, in Fig. 3 we plot the area enclosed between the meandering stream and its centerline as a function of downstream distance. The deviation of the model from the power law is likely due to the length scale associated with the forcing (characteristic droplet size 1-5 mm). The area grows as $x^{7/4} = x^{1.75}$ with the distance, consistent with the power law $k^{-5/2}$ of the spectrum. Surprisingly, it is *the same* growth law for the growth of the area of a river basin versus length of the river discovered by Hack (1957). In our case, there is clearly no basin *per se* and no side streams forming that basin. We deliberately avoid plotting Hack's law data for rivers on the same graph here for fear of misleading the reader into thinking that our experiment is describing river basin erosion. However, an overlap of the properly scaled data for Hack's law in Fig. 3 with the river data from Rigon *et al.* (1996) would be nearly perfect.

Thus we can conclude that the behavior of a stream meandering down an inclined plane is dominated by the effects of the stream interacting with droplets on the plane, which can be modeled by including appropriate random forcing into the equations.

5. Sketch of stochastic solution for (3.2–3.4)

It is interesting to compare the numerical results of the model with the exact analytical solution in stochastic sense for (3.2–3.4), which we will now sketch briefly. Following previous argument, we assume that the noise is quenched, or colored, just as in turbulence. This implies that both u and v scale as the solutions of the noise-driven Navier-Stokes equation in one-dimensional turbulence, see Birnir (2007). A typical Reynolds number value for our experiment is about 4500, but in extreme cases it can vary from as low as 500 (water replaced with glycerin, small fluxes) to 18000 (water, large fluxes).

The stochastic solution proceeds as follows. First, we assume h_t in (3.4) to be negligible compared to uh_x and v. Then we get $h_x = v/u$. We define second-order structure functions $s_f = \int |f(x+\ell) - f(x)|^2 dx$ as in Frisch (1995); Birnir *et al.* (2007) and assume scaling $s_h \sim \ell^{2p_h}$, $s_u \sim \ell^{2p_u}$ and $s_v \sim \ell^{2p_v}$. Then the powers are related as $p_h = p_v - p_u + 1$. We can disregard the lubrication friction terms in (3.2,3.3) by setting $\lambda = 0$, and setting η to be white noise. Then, the u equation (3.2) is simply a noise-driven Burgers equation which can be solved exactly, giving $p_u = 3/2$. On the other hand, (3.3) can be solved exactly under these assumptions using the Feynman-Kac technique as in Simon (2005), yielding $p_v = 2/3$, and from the equation for p_h we conclude that $p_h = 1/6$.

Sadly, in our case setting any realistic value of $\lambda > 0$ in (3.2,3.3) destroys the scaling
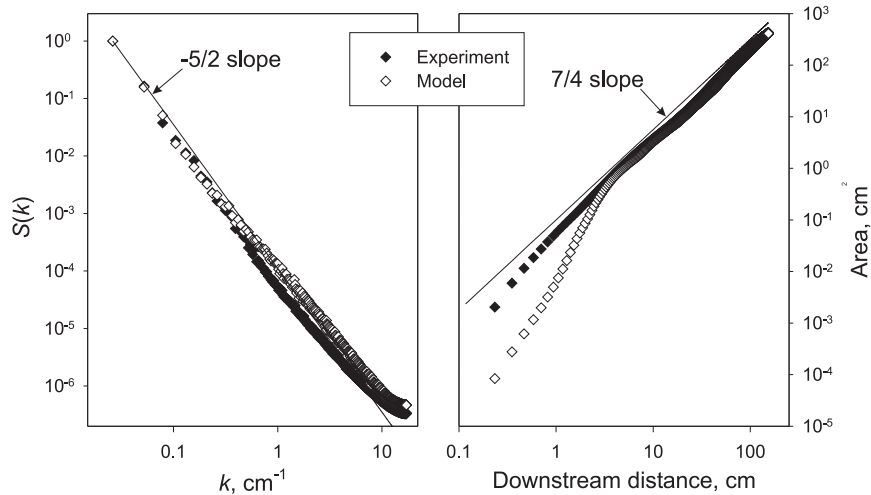
FIGURE 3. Comparison of experiments and theory (experimental data for acrylic surface used). Left: Power spectra of the deviation of the stream from the centerline. Solid line represents $\alpha = -5/2$ power law. The noise amplitude in the model (a universal constant for all experiments) is fixed to achieve agreement at small wavenumbers k, which continues over all the k values having physical relevance. Right: Area enclosed between the stream and the centerline as the function of downstream distance. Solid line shows power law with exponent $7/4 = 1.75$. The deviation of the model from experiment is observed for distances comparable to the width of noise forcing, equal to the diameter of the stream.

$p_h = 1/6$. Also, numerics show that the characteristic time for the system to evolve $p_h = 1/6$ scaling for any realistic initial conditions is so large that it can only be observed after several km downstream. It is nevertheless interesting that the meandering exponent $p_h + 1 \simeq 1.16$ agrees with that of mature rivers $(1.1 - 1.2)$. It was shown recently that the river meandering exponent is fundamental and all other exponent in Earth's morphology can be derived from it, see Dodds & Rothman (1999, 2000a,b,c). These curious coincidences between our experiments and models with real river morphology warrant further investigation.

6. Conclusions and further directions

In this paper, we demonstrate that meandering of a fluid stream on a partially hydrophobic surface is caused exclusively by the presence of disturbances in the flow rate and is maintained by the presence of droplets left behind by a meandering stream. We derive a model from the first principles that provides an accurate description of the stochastic behavior of the stream. Interestingly enough, some of the results of the model fit not only our simple experiment, but also well-established results for river morphology. In particular, the basin of rivers versus river's length and the unsigned area between the centerline versus position grow with exactly the same exponent, $7/4$. In addition, the meandering exponent for our model (3.2-3.4) with the white noise for η and no friction dissipation (*i.e.*, $\lambda = 0$) corresponds to the meandering of rivers.

10   *B. Birnir, K. Mertens, V. Putkaradze, and P. Vorobieff*

REFERENCES

BIRNIR, B. 2007 Turbulent rivers. *Nonlinearity* **(under consideration)**.

BIRNIR, B., HERNANDEZ, J. & SMITH, T.R. 2007 The stochastic theory of fluvial landsurfaces. *J. Nonlinear Sci.* **17**, 13–57.

BIRNIR, B., MERTENS, K., PUTKARADZE, V. & VOROBIEFF, P. 2008 Noise driven meandering streams. *Physical Review Letters* **(under consideration)**.

CLANET, C. 2000 Clepsydrae from Galileo to Torricelli. *Phys. Fluids* **12**, 2743–2751.

CULKIN, J.B. & DAVIS, S.H. 1984 Meandering of water rivulets. *AIChE J.* **30**, 263–267.

DAVIS, S.H. 1980 Moving contact lines and rivulet instabilities. 1. The static rivulet. *J. Fluid Mech.* **98**, 225–242.

DEGENNES, P.G. 1985 Wetting: statics and dynamics. *Rev. Mod. Phys.* **57**, 827–863.

DODDS, P.S. & ROTHMAN, D. 1999 Unified view of scaling laws for river networks. *Phys. Rev E* **59**, 4865–4877.

DODDS, P.S. & ROTHMAN, D. 2000a Geometry of river networks. I. Scaling, fluctuations, and deviations. *Phys. Rev E* **63**, 016115.

DODDS, P.S. & ROTHMAN, D. 2000b Geometry of river networks. II. Distributions of component size and number. *Phys. Rev E* **63**, 016116.

DODDS, P.S. & ROTHMAN, D. 2000c Geometry of river networks. III. Characterization of component connectivity. *Phys. Rev E* **63**, 016117.

FRISCH, U. 1995 *Turbulence*. Cambridge, UK: Cambridge University Press.

HACK, J. 1957 Studies of longitudinal stream profiles in Virginia and Maryland. *U.S. Geological Survey Professional Paper* **294-B**.

IKEDA, S., PARKER, G. & SAWAI, K. 1981 Bend theory of river meanders. 1. Linear development. *J. Fluid Mech.* **112**, 363–377.

KIM, H.-Y., KIM, J-H. & KANG, B.H. 2004 Meandering instability of a rivulet. *J. Fluid Mech.* **498**, 245–256.

LE GRAND-PITEIRA, N., DAERR, A. & LIMAT, L. 2006 Meandering rivulets on a plane: A simple balance between inertia and capillarity. *Phys. Rev. Lett* **96**, 254503.

LEOPOLD, L.B. & WOLMAN, M.G. 1960 River meanders. *Bull. Geol. Soc. Am.* **71**, 769–793.

MERTENS, K., PUTKARADZE, V. & VOROBIEFF, P. 2004 Braiding patterns on an inclined plane. *Nature* **430**, 165.

MERTENS, K., PUTKARADZE, V. & VOROBIEFF, P. 2005 Morphology of a stream flowing down an inclined plane. Part 1. Braiding. *J. Fluid Mech.* **531**, 49–58.

NAKAGAWA, T.M.S. 1992 Rivulet meanders on a smooth hydrophobic surface. *Int. J. Multiphase Flow* **18**, 455–463.

NAKAGAWA, T.M.S. & NAKAGAWA JR., R. 1996 A novel oscillation phenomenon of the water rivulet on a smooth hydrophobic surface. *Acta Mechanica* **115**, 27–37.

NAKAGAWA, T. & SCOTT, J.C. 1984 Stream meanders on a smooth hydrophobic surface. *J. Fluid Mech.* **149**, 89–99.

RIGON, R., RODRIGUEZ-ITURBE, I., MARITAN, A., GIACOMETTI, A., TARBOTON, D. G. & RINALDO, A. 1996 On Hack's law. *Water Resources Research* **32**, 3367–3374.

SCHMUKI, P. & LASO, M. 1990 On the stability of rivulet flow. *J. Fluid Mech.* **215**, 125–143.

SEMINARA, G. 2006 Meanders. *J. Fluid Mech.* **554**, 271–297.

SIMON, B. 2005 *Functional Integration and Quantum Physics, 2nd ed.*. AMS Chelsea Publishing.

WEILAND, R.H. & DAVIS, S.H. 1981 Moving contact lines and rivulet instabilities. 2. Long waves on flat rivulets. *J. Fluid Mech* **107**, 261–280.

YOUNG, G.W. & DAVIS, S.H. 1987 Rivulet instabilities. *J. Fluid Mech* **176**, 1–30.